Design and Implementation of Capacitive Micromachined Ultrasonic Transducers for High Power

F. Yalcin Yamaner[1], *Member, IEEE*, Selim Olcum[2], *Member, IEEE*, Ayhan Bozkurt[1], *Member, IEEE*, Hayrettin Köymen[2], *Senior Member, IEEE* and Abdullah Atalar[2], *Fellow, IEEE*

[1] Sabanci University, Electronics Engineering, Istanbul, Turkey
[2] Bilkent University, Electrical and Electronics Engineering Department, Ankara, Turkey

***Abstract*— Capacitive micromachined ultrasonic transducers (CMUTs) have a strong potential to compete piezoelectric transducers in high power applications. In a CMUT, obtaining high port pressure competes with high particle velocity: a small gap is required for high electrostatic force while particle displacement is limited by the gap height. On the other hand, it is shown in [1] that CMUT array exhibits radiation impedance maxima over a relatively narrow frequency band. In this paper, we describe a design approach in which CMUT array elements resonate at the frequency of maximum impedance and have gap heights such that the generated electrostatic force in uncollapsed mode, can sustain particle displacement peak amplitude up to the gap height. The CMUT parameters are optimized for around 3 MHz of operation, using both a SPICE model and FEM. The optimized parameters require a thick membrane and low gap heights to get maximum displacement without collapsing membrane during the operation. We used anodic bonding process to fabricate CMUT arrays. A conductive 100 μm silicon wafer is bonded to a glass wafer. Before the bonding process, the silicon wafer is thermally oxidized to create an insulating layer which prevents break down in the operation. Then, the cavities are formed on the insulating layer by a wet etch. The gap height is set to 100 nm. Meanwhile, the glass wafer is dry etched by 120 nm and the etched area is filled by gold evaporation to create the bottom electrodes. The wafers are dipped into piranha solution and bonding process is done afterwards. The fabricated CMUTs are tested in an oil tank. To eliminate the DC voltage which may cause charging problem in the operation, we tried to drive the CMUT array with large continuous wave signals at half of the operating frequency. We observed 1MPa peak to peak pressure with -23 dB second harmonic at the surface of the array (Fig. 1). The proposed design further extends the operation of CMUTs. Observing low harmonic distortions at high output pressure levels, without any charging problem, make CMUT a big candidate for high power applications.**

I. INTRODUCTION

Capacitive micromachined ultrasonic transducer has been introduced in 1996 [2] and since then it has been a hot topic for the research groups as an alternative technology to piezoelectricity. As the technology is investigated and new prototypes are introduced, CMUT became a strong competitor of piezoelectric materials. The benefit of silicon micromachining provide the easy integration of CMUT to CMOS process and enable the miniaturization of the technology. The disadvantages of high electrical field requirement is eliminated by proposed fabrication and operating methods [3], [4]. Recently, the technology is proposed to be used in the treatment of tumors by high intensity focused ultrasound (HIFU) [5]. In a HIFU operation, the transducer is driven by continuous wave signals to heat the targeted tissue for the time required by the treatment. The initial experiments present that CMUT is an alternative candidate for HIFU operation and the technology can be used for the operation. In this paper, we show that CMUT performance under continuous wave drive signal can be maximized by considering the radiation impedance of the transducer and operating transducer where transducer sees the maximum radiation impedance.

The nonlinear electrical circuit model in [6] is used for the optimization. First, the circuit is improved by including a realistic radiation impedance model of CMUT array, then the accuracy of the circuit is increased by further modification on circuit parameters by doing finite element simulations.

CMUTs were fabricated with high membrane thickness and low gap heights using anodic bonding technology. The important charge trapping issue in CMUT operation has been eliminated by driving CMUTs at half the operating frequency without a DC voltage. It has been shown that a DC voltage bias is not necessary for transmit operation to obtain high output pressure levels.

II. NONLINEAR SPICE MODEL FOR UNCOLLAPSE MODE OF CMUT

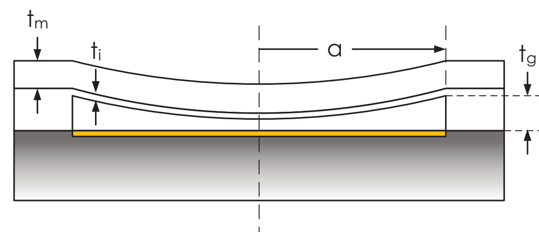

Fig. 1. Representative cross section of a circular membrane with radius a, thickness t_m and gap height of t_g. Top electrode is the conductive silicon wafer.t_i is the insulating layer thickness above the gap. The bottom electrode is a metal layer.

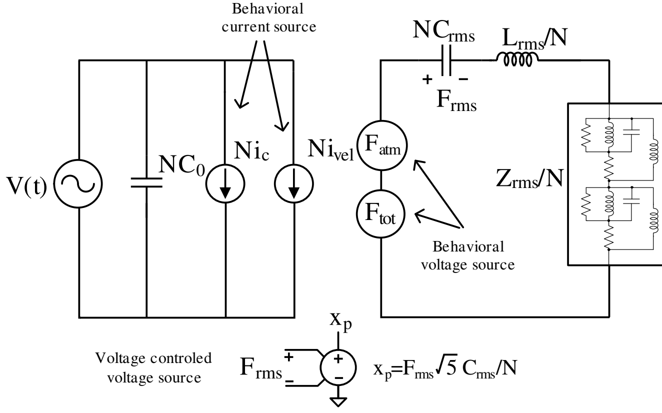

Fig. 2. SPICE model of CMUT operating in uncollapse mode.

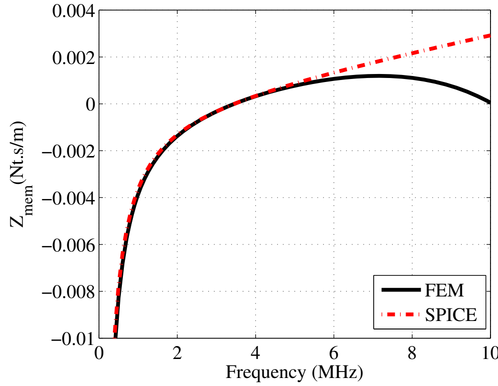

Fig. 3. The resonant frequency of the membrane as determined from L_{rms} and C'_{rms} for various t_m/a values. C'_{rms} is the corrected capacitor value to accurately model resonant frequency. Membrane impedance is plotted for a radius of 280 μm and a membrane thickness of 92 μm.

The CMUT is highly nonlinear when used as a transmitter, hence a model capable of handling nonlinear effect is required [7]. The nonlinear electrical circuit model of an immersed circular CMUT depicted in [6] is used as the basis of the SPICE model in this paper. The model is created by K. Oguz, et al. and the performance of the model is demonstrated using a harmonic balance simulator. The model is carried into a SPICE environment in order to do transient simulations (Fig. 2). C_0 in the electrical port represents the undeflected capacitance of the transducer, i_c represents the current caused by additional capacitance due to deflection, and i_{vel} is the current generated by the mechanical movement. The mechanical side is modeled using lumped parameters. We preferred the root mean square (rms) velocity instead of the average velocity as the lumped through variable. The lumped parameters, C_{rms} and L_{rms} accurately model the membrane resonant frequency for $t_m/a < 0.1$ [8]. To maintain the accuracy of the model for thick membranes, a correction term is added to the C_{rms}. With the corrected value, the model is fully consistent with FEM for $t_m/a = 0.8$. (Fig. 3).

$$C_{rms_{corrected}} = C_{rms}(1.019 + 5.005(\frac{t_m}{a})^{1.981}) \quad (1)$$

When CMUT operates in air, the effect of atmospheric pressure must be included in the model. The effect can be easily included in the model by adding an extra force term into the total force equation at the mechanical side. This force term is written in terms of the atmospheric pressure multiplied by the surface area and the rms correction factor [6].

$$F_{atm} = \frac{\sqrt{5}}{3} P_{atm} \pi a^2 \quad (2)$$

The x_p values are predicted for different dc voltages, and compared to FEM results (Fig. 4).

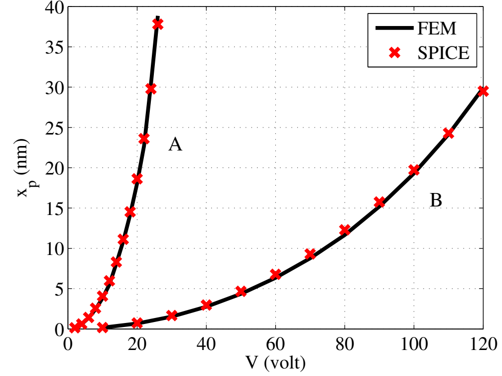

Fig. 4. The static deflection of membrane center as calculated by FEM and the circuit model ($a = 30$ μm, t_m=2 μm, t_i=0.1 μm, t_g=0.1 μm (A). $a = 300$ μm, t_m=100 μm, t_i=0.4 μm, t_g=0.1 μm (B).)

The circuit proposed in [9] is created to model the frequency depended radiation impedance of the array. The created R, L, C network accurately models the radiation impedance and provides realistic simulations of the arrays in a fluid medium. The component values are defined in relation to the radius (a), the sound velocity in the medium (c), the density of the medium (ρ_0) and, the number of cells in the array (N). Thus, the model accurately mimics the radiation impedance in any case of a change in the related parameters.

We created the subcircuit in Fig. 5 that accurately models the radiation impedance of the proposed array.

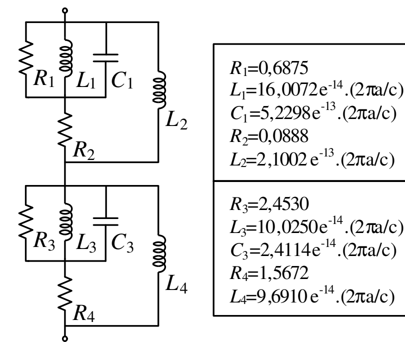

Fig. 5. RLC model for the normalized radiation impedance (Z_{rms}/N) of a CMUT array.

III. Optimization of CMUT Parameters

For a CMUT operating under a continuous wave signal, it is possible to eliminate the DC voltage at the input. This can

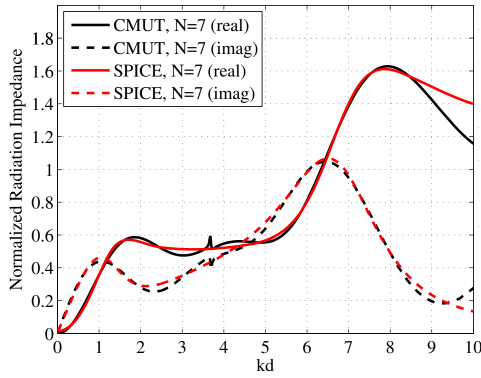

Fig. 6. The normalized radiation impedance of a CMUT array of 7 cells

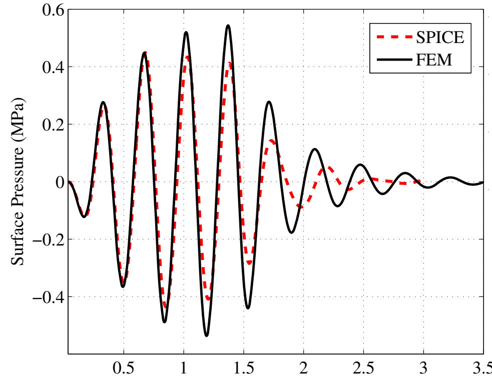

Fig. 7. Observed surface pressure. 2 cycle 100Vpeak cosine burst at 1.44 MHz is applied to CMUT element with 7 cells under fluid loading (a=280 μm, t_m=92 μm, t_g=110 nm, t_i=350 nm.)

be done by applying a sinusoidal signal with a frequency at half of the operating frequency. If the applied drive voltage is

$$V(t) = V_{max}\cos(\frac{\omega}{2}t + \theta) \tag{3}$$

where V_{max} is the peak voltage, then F, the force on the membrane, will be proportional to

$$F \propto V^2(t) = \frac{V_{max}^2}{2}[1 + \cos(\omega t + 2\theta)] \tag{4}$$

As seen in Eq. 4, $V^2(t)$ includes a DC term that will naturally form a bias voltage and a sinusoidal force term at the operating frequency. Therefore, the mechanical effect of the DC voltage can be achieved by using a continuous wave signal at half of the operating frequency.

We targeted an operation of 3 MHz and optimize our CMUT parameters accordingly. We assumed that our available drive circuitry can provide 100V peak voltage to transducers. The insulating layer thickness is chosen as 200nm to prevent breakdown in the insulating layer during the operation.

The radiation impedance peak of an array of 7 cells is at $ka = 3.75$. Thus, the radius to observe the maximum radiation impedance at this frequency is 298.4μm. Using the circuit model, we found the t_m parameter as 130μm for a resonance at 3 MHz. Then we continuously applied 100V_p cosine signal at half of the resonant frequency (1.5 MHz) and reduce t_g from a high value while monitoring the peak displacement. At a point, x_p value gets close to t_g which means that membrane starts to touch the bottom electrode. At a t_g value of 84nm the center peak displacement is found as 80nm. As t_g gets smaller, the resonance frequency shifts due to spring softening. In order to adjust the resonance frequency the membrane thickness is increased and the last step is repeated. After a few iteration, t_m and t_g values are found as 125μm and 81nm, respectively.

IV. Fabrication

The wafer bonding technology enables more control over the CMUT fabrication process [4]. Gap height can be defined precisely. Moreover, the membrane thickness is no more limited by the deposition; the wafer itself is used as a membrane or a predefined membrane layer is transferred. For the fabrication of a high power CMUT transducer, we utilized anodic wafer bonding. Anodic bonding is used to bond a silicon wafer to a borosilicate wafer using proper pressure, electric field and temperature. The cavities and the insulating layer are formed over the silicon wafer and the bottom electrode is defined over the borosilicate wafer.

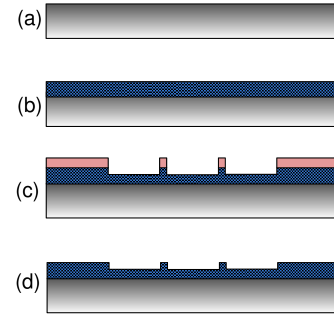

Fig. 8. (a)3 inch Conductive silicon wafer with a thickness of 100 μm. (b) Thermal oxidation (c) Lithography and oxide etching to form the cavities

Fig. 8 shows the process over the silicon wafer. We used 3 inches, highly doped, double side polished silicon wafer. The wafer is highly conductive (0.015-0.020 ohm-cm), thus it serves as one of the electrodes of the CMUTs. The thickness of the silicon wafer determines the thickness of the membrane which is 100 μm. To create an insulation layer, 450 nm silicon oxide is thermally grown using a diffusion furnace. The cavities are formed over the insulating layer by etching 100 nm of silicon oxide.

On the other hand, a 3.2 mm thick 4 inches borosilicate wafer is used as a substrate (Fig. 9). The bottom electrodes are formed over this non conductive substrate. The borosilicate wafer is etched with RIE using an image reversal photoresist as a mask. The etched areas are than filled by gold evaporation. This step is critical for bonding and determining the overall gap height. We continuously monitored the thickness of gold during evaporation. Before the bonding process, the borosilicate and silicon wafers are dipped into Piranha solution. The prepared wafers are then anodic bonded[1].

[1]Applied Microengineering Ltd, Oxfordshire, UK.

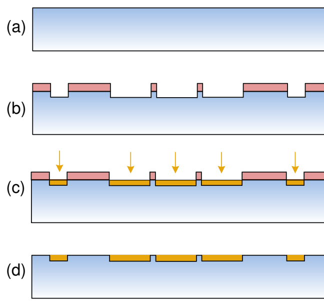

Fig. 9. (a)Borosilicate glass wafer (b)Lithography and glass etching for bottom electrode (c)Ti/Au deposition (d)Cleaning

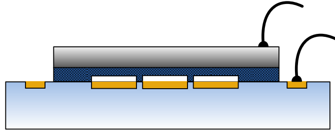

Fig. 10. After anodic bonding, lead wires are connected using conductive epoxy.

V. Experimental Results

The tested CMUT element properties is given in Table I. The element consist of 19 CMUT cells and the total capacitance including the paths is measured as 280 pF. Immersion

membrane radius, a	280μm
membrane thickness, t_m	100μm
insulating layer, thickness, t_i	$Si0_2$, 350nm
gap height, t_g	100nm

TABLE I
THE PARAMETERS OF THE TESTED CMUTS ON GLASS WAFER.

experiments were done in a vegetable oil tank. Signal generator output is amplified by using ENI 2100 100W Class A Linear Power amplifier. The amplifier has a fixed nominal gain of 50dB. The amplified 6 cycle cosine burst signal at 1.15 MHz is applied to the transducer element. An HGL-200 calibrated ONDA hydrophone is placed 1 cm away from the transducer surface. The measured signal is corrected for the diffraction and attenuation losses to obtain the surface pressure (Fig. 11). We observed 1MPa surface pressure with -23dB second harmonic at the transducer surface.

VI. Conclusions

The proposed model can be used to accurately simulate the behavior of a CMUT for the uncollapsed region. The uncollapsed region is suitable for low harmonic high power applications. The parameters can be optimized in a fast way as compared to FEM. Furthermore, the circuit can be used as a CMUT front-end IC test bench to optimize the ICs performance before fabrication. Higher radiation impedance improves the transducers performance. For the given voltage and for the given total transducer area, the cMUT cell radius should be chosen to maximize the radiation resistance at the operating frequency to get high power.

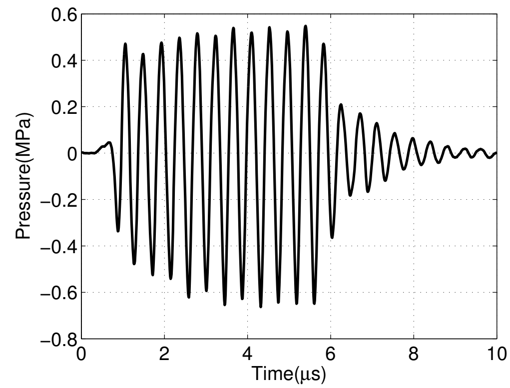

Fig. 11. 6 cycle 150Vpeak cosine burst at 1.15 MHz is applied to the CMUT element. 1.18 MPa surface pressure is observed.

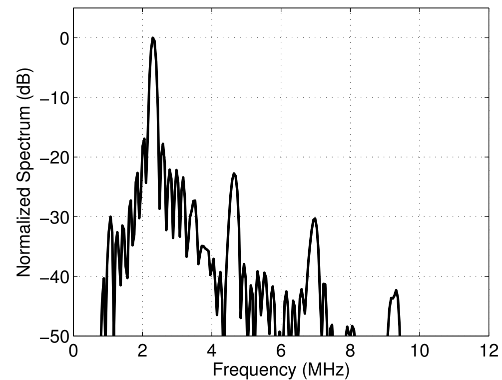

Fig. 12. Normalized frequency spectrum of the surface pressure

References

[1] M. N. Senlik, S. Olcum, H. Köymen, and A. Atalar, "Radiation impedance of an array of circular capacitive micromachined ultrasonic transducers," *IEEE Trans. Ultrason., Ferroelect., Freq. Contr.*, vol. 57, pp. 969–976, 2010.

[2] M. I. Haller and B. T. Khuri-Yakub, "A surface micromachined electrostatic ultrasonic air transducer," *IEEE Trans. Ultrason., Ferroelect., Freq. Contr.*, vol. 43, pp. 1–6, 1996.

[3] B. Bayram, Ö. Oralkan, A. S. Ergun, E. Hæggström, G. G. Yaralioglu, and B. T. Khuri-Yakub, "Capacitive micromachined ultrasonic transducer design for high power transmission," *IEEE Trans. Ultrason., Ferroelect., Freq. Contr.*, vol. 52, pp. 326–339, 2005.

[4] K. K. Park, H. Lee, M. Kupnik, and B. Khuri-Yakub, "Fabrication of capacitive micromachined ultrasonic transducers via local oxidation and direct wafer bonding," *Microelectromechanical Systems, Journal of*, vol. 20, no. 1, pp. 95 –103, feb. 2011.

[5] S. H. Wong, R. D. Watkins, M. Kupnik, K. B. Pauly, and B. T. Khuri-Yakub, "Feasibility of MR-temperature mapping of ultrasonic heating from a CMUT," *IEEE Trans. Ultrason., Ferroelect., Freq. Contr.*, vol. 55, pp. 811–818, 2008.

[6] H. K. Oguz, S. Olcum, M. N. Senlik, V. Tas, A. Atalar, and H. Köymen, "Nonlinear modeling of an immersed transmitting capacitive micromachined ultrasonic transducer for harmonic balance analysis," *IEEE Trans. Ultrason., Ferroelect., Freq. Contr.*, vol. 57, pp. 438–447, 2010.

[7] A. Lohfink and P. C. Eccardt, "Linear and nonlinear equivalent circuit modeling of CMUTs," *IEEE Trans. Ultrason., Ferroelect., Freq. Contr.*, vol. 52, pp. 2163–2172, 2005.

[8] H. Köymen, M. N. Senlik, A. Atalar, and S. Olcum, "Parametric linear modeling of circular CMUT membranes in vacuum," *IEEE Trans. Ultrason., Ferroelect., Freq. Contr.*, vol. 54, pp. 1229–1239, 2007.

[9] F. Y. Yamaner, S. Olcum, H. K. Oguz, A. Bozkurt, H. Koymen, and A. Atalar, "Optimizing cmut geometry for high power," in *Proc. IEEE Ultrason. Symp.*, 2010, pp. 2247–2250.